Fuel 170 (2016) 16–26

Contents lists available at ScienceDirect

Fuel

journal homepage: www.elsevier.com/locate/fuel

Fouling propensity of high-phosphorus solid fuels: Predictive criteria and ash deposits characterisation of sunflower hulls with P/Ca-additives in a drop tube furnace

L. De Fusco [a,*], A. Boucquey [a], J. Blondeau [c], H. Jeanmart [a], F. Contino [b,d]

[a] Institute of Mechanics, Materials, and Civil Engineering (iMMC), Université catholique de Louvain, Place du levant 2, 1348 Louvain-la-Neuve, Belgium
[b] Department of Mechanical Engineering, Vrije Universiteit Brussel, Pleinlaan 2, 1050 Brussels, Belgium
[c] Laborelec, Rodestraat 125, 1630 Linkebeek, Belgium
[d] Combustion and Robust Optimization Group (BURN), Université Libre de Bruxelles and Vrije Universiteit Brussel, Bruxelles, Belgium

HIGHLIGHTS

- We propose a characterisation tool to describe the fouling of high-P solid fuels.
- The influence of H_3PO_4 and $CaCO_3$ additives is studied in a drop tube furnace.
- Visual and SEM–EDX analyses are applied to the deposits.
- A proper addition of Ca-, P-based additives can reduce the sunflower hulls fouling.
- The experimental results confirm the added value of the characterisation approach.

ARTICLE INFO

Article history:
Received 18 April 2015
Received in revised form 8 December 2015
Accepted 10 December 2015
Available online 22 December 2015

Keywords:
Sunflower hulls
Phosphorus
Fouling
Drop tube furnace

ABSTRACT

Fouling from the processing of residual biomass fuels in combustion applications is a major concern. This paper discusses the fouling behaviour of sunflower hulls with a high phosphorus (P) content by means of a broad fuel characterisation strategy including advanced predictive indices, the fuel selective leaching, multiple deposition tests in a Drop Tube Furnace (DTF) and deposits analysis with scanning electron microscopy–energy dispersive X-rays spectroscopy (SEM–EDS). First, we summarise the P-role in the ash chemistry, with a focus on the fouling mechanisms. Second, a characterisation strategy of the ash, based on three indices, including some details from the fuel selective leaching, is proposed to describe the P-rich fuels propensity to foul. The developed approach could be used as a complement to chemical equilibrium models. Thirdly, the characterisation strategy is applied to sunflower hulls. Deposition tests in an industrial scale DTF are performed for the raw fuel, and for the fuel with phosphoric acid (H_3PO_4) water solution and calcium carbonate ($CaCO_3$) as additives, to obtain different P/K and P/Ca ratios in the fuel composition. The results show that increasing the fuel P-content allows to capture the alkali metals in alkali–alkaline earths–phosphates and alkali–phosphates phases, reducing the occurrence of deposits of S- and Cl-compounds. Low melting temperature phases can be reduced enhancing the formation of coarser, high melting temperatures ash particles formed by K/Na–Ca/Mg–phosphates, by means of an optimised addition of phosphorus- and active calcium-based additives. The experimental results confirmed the added value of the high-P fuels predictive characterisation strategy.

1. Introduction

Biomass is one of the renewable energy sources that are envisaged to be intensively used in a new energy paradigm. Because of woody biomass decreasing availability, a growing interest is observed for herbaceous biomass and agricultural residues, such as straws, husks and hulls, to be used as a fuel, both in small scale and large-scale production plants. As an example, in southern Europe, a total of 2.66 million hectares of sunflower are grown each year, mainly for oil production, evidencing the potential energy utilisation of the residues from the de-hulling, which is practised prior to the oil-extraction process [1]. Nevertheless, the combustion of these fuels portends several ash related issues such as slag

* Corresponding author. Tel.: +32 10472219.
E-mail address: lucio.defusco@uclouvain.be (L. De Fusco).

http://dx.doi.org/10.1016/j.fuel.2015.12.017
0016-2361/

formation, bed agglomeration, fouling and corrosion [2,3]. Among the ash related issues, fouling is mainly driven by a volatilisation–condensation mechanism of low-melting point inorganic species [3–6].

Fouling is primarily influenced by the fuel inorganic composition, which can vary greatly, then by the boiler design and the operating conditions (i.e. the temperature profile along the boiler) [7–9]. First the alkalis (K, Na) and alkaline earth metals (Ca, Mg), then Si, S, Al, P and Cl are present in substantial amounts in biomass fuels (Table 1) and are significant to fouling mechanisms [6,9–11].

In herbaceous fuels the potassium content can exceed 1 wt.% (on weight on a dry basis) (Table 1), essentially occurring as highly volatile ionic salts [2,9–11], which can react during the combustion to form different alkali compounds in the deposits: alkali phosphates, hydroxides, carbonates, silicates, chlorides, sulphates. As an example, sunflower hulls have noticeable sulphur and chlorine contents, with a high risk of sulphates condensation and Cl-induced corrosion [12]. Ash salt mixtures including K, Na, S, Cl have a melting temperature of approximately 600 °C, which can decrease when including heavy metals such as Pb and Zn [13].

Phosphorus (P) can be present in large amounts in several herbaceous biomass fuels such as rapeseed cake, distillers dried grains with solubles (DDGS), bran, corn stover, oat straw and sunflower hulls (Table 1). In the recent years, because of its considerable influence on the fouling mechanisms [14,15], an increasing interest has been given to the influence of phosphorus on ash formation and deposition: several experiments were conducted by Piotrowska [14], Eriksson [16], Grimm [15], Billen et al. [17], Wu et al. [18]. The fuels investigated were rapeseed cake pellets, wheat straw, logging residues, DDGS, poultry litter and bran.

Chemical fractionation analyses on a P-rich fuel show that it is present in the fuel in different associations, having different reactivities during combustion [14,15]. Mineral phosphorus is usually not much reactive while organic phosphorus has a higher reactivity [19]. In woody fuels, it is mainly inorganically bound, therefore most of P is embedded in the coarse fly ash fraction. In agro-fuels and biogenic residues, a share of P may be organically bound, participating in the gas phase reactions and aerosol formation process [13].

During combustion, phosphorus compounds are released out as $P_2O_5(g)$. This species can then either form low melting points alkali phosphates salt particles (e.g. K_3PO_4, $K_5P_3O_{10}$ and KPO_3) according to Eq. (1) [20], or react with calcium compounds to form stable and solid calcium phosphates [21] (Table 2), as an example according to Eq. (2) [20]. Besides, alkali phosphates are rather volatile and can react with alkaline earth metals to form solid ternary phosphates belonging to the K_2O—CaO—P_2O_5 system, which have melting points above 1000 °C [22] (Table 2). A plausible global reaction, see Eq. (3), was proposed by Wu et al. [18].

$$P_2O_5(g) + 2KOH(g) \rightleftharpoons 2KPO_3(l,g) + H_2O(g) \quad (1)$$

$$P_2O_5(g) + 2CaO(s) \rightleftharpoons Ca_2P_2O_7(s) \quad (2)$$

$$KPO_3(l,g) + CaO(s) \rightleftharpoons KCaPO_4(s) \quad (3)$$

When available, phosphorus will tend to react with alkali before any alkali chlorides, alkali sulphates or alkali hydroxides can form [15]. According to Boström [20], if equilibrium is attained, K–phosphates will be the first species to form followed by K–sulphate, K–chloride, K–carbonate and K–hydroxide. According to the same authors, P also dominates over Si in the competition for the base cations: K^+, Mg^{2+} and Ca^{2+}; thus K–Mg/Ca phosphates form prior to the corresponding silicates. However, Billen et al. [23] state that not all phosphates are thermodynamically more stable than silicates.

Table 1
Order of magnitude for some inorganic element concentrations (in fuel dry weight percentage) for some selected fuels (Phyllis 2, ECN).

	Woody fuel	Herbaceous fuel	Sunflower hulls (%)[a]
K + Na	~0.1%	~2%	~1.6
Ca + Mg	Variable	Variable	~0.8
Si	~0.2%	~0.2 ... 4%	~0.3
Cl	~0.1%	~0.2 ... 3%	~0.2
P	~0.1%	~0.2 ... 2%	~0.4

[a] Average from sample analyses.

Table 2
Melting behaviour of some compounds from the ternary diagram K–Ca–P [14,24,25].

Compound	Melting T (°C)	P/K	P/Ca
KPO_3	810	1	–
$KCa(PO_3)_3$	846	3	3
$Ca(PO_3)_2$	984	–	2
$K_4P_2O_7$	1105	0.5	–
$CaK_2P_2O_7$	1143	1	2
$Ca_2P_2O_7$	1353	–	1
$KCaPO_4$	1560	1	1
$Ca(PO_4)_2$	1670	–	2

Experimental results [14–16] showed that phosphorus-rich fuels can decrease the problems related to fouling by converting the low melting temperature alkali species present in the gas phase – probably alkali oxides or hydroxides that are formed during the initial combustion stages – into high melting temperature alkali–alkaline earth–phosphates: K/Na–Ca/Mg–phosphate[1] will essentially form coarse fly ash particles while the amount of fine fly ash is reduced. Grimm [19] underlines that phosphorus could be used as an additive to form ternary phosphates, such as $CaK_2P_2O_7$, provided that sufficient active calcium additives (e.g. organically bound or dissolved calcium compounds) are available, mitigating the alkali phosphates formation [15,16].

However, under high phosphorus concentrations and low alkaline earth metal concentrations in the fuel, low melting temperature alkali phosphates are formed on top of the K–Ca–phosphate ternary phase, causing an increase in the fouling propensity of the fuel [15]. In the ternary diagram K–Ca–P, these compounds are situated near the region where KPO_3 is found. Also, Billen et al. [17] evidenced that high phosphorus concentrations can cause melt formation (during fluidized bed combustion) not because of the formation of low melting points alkali phosphates, but because Ca–phosphates instead of Ca–silicates are formed, with consequent availability of silicates to form low melting points K–silicates.

Although some investigations have been carried out, more work is needed to understand additional details of the phosphorus role in the ash chemistry of agricultural residues combustion. Theoretical models based on equilibrium calculations still suffer from the lack of data and from results dependency on the database used for the phosphorus compounds [13,18,23].

The objectives of this work are: (i) develop a semi-empirical characterisation strategy for high-P fuels based on present knowledge (ii) perform experimental testing of sunflower hulls fuel combustion: qualitatively characterise the fuel deposition propensity based on the strategy developed and study the sunflower hulls fouling deposition behaviour by means of combustion tests in a

[1] Sodium is expected to have a similar behaviour as potassium. Even though K–Mg–phosphates are expected to react in a similar way as K–Ca–phosphates, it seems that Mg is much weaker to retain P compared to Ca. This can be seen comparing the melting temperatures of the formed compounds. The K–Mg–P phase diagram can be found in [26].

Drop Tube Furnace (DTF). The combustion tests are performed in presence of additives (phosphoric acid and calcium carbonate) to explore different P/K and P/Ca molar ratios in the fuel composition. SEM–EDX analyses are applied on the DTF deposits.

The simplified characterisation strategy and the experimental set up are described in Section 2. The results of the fuel characterisation (i) and the outcome of the experimental testing (ii) are discussed in Section 3.

2. Methodology and materials

2.1. High phosphorus fuels characterisation strategy

Some slagging and fouling indices proposed in the literature can be considered as valuable means for a first assessment of the ash deposition propensity for a given fuel. Typical indices based on the inorganic fuel composition were selected from the literature [27–29] and reported in Table 3. They hardly account for the influence of P in the deposition mechanisms.

More advanced strategies have been proposed. Grimm [15] suggested that the relationship $(K + Na)/(Ca + Mg)$ in the overall fuel ash should be considered to evaluate the possibility of fouling reduction using active phosphorus as additive. Novakovic and co-authors [31], studying the K–Ca–P ash system, evidenced that a decreased Ca/P molar ratio significantly decreased the K-volatilisation rate. Piotrowska [24] showed that when the Ca/P ratio is larger than 1 and the $(K + Na)/(Ca + Mg)$ ratio is smaller than 1, sintering issues in fluidized bed combustion are not evidenced.

Søresen et al., studying straw combustion in presence of mixed P and Ca-based additives, reported a reduction of 74–98% of the level of Cl in the deposits when the molar ratios of P/(K + Na) and P/Ca in the resulting fuel were in the ranges 1.9–3.2 and 0.8–0.9, respectively [25,32,33]. The amount of P and Ca to be added, should be [32]:

$$\frac{P_{added} + P}{K + Na - Cl} \geqslant 1 \quad (4)$$

$$\frac{P_{added} + P}{Ca_{added} + Ca} \leqslant 2 \quad (5)$$

where K, Na, P, Ca, Cl are the elements molar quantities in the fuel ash. The presence of chlorine in the first ratio is because Cl is expected to capture the potassium in KCl compounds [32]. Concerning the second relation, according to Søresen et al., in order to obtain $KCaPO_4$ (Table 2) as the major product, Ca, P and K should be present in equal molar amounts; to obtain $K_2CaP_2O_7$ (Table 2) as the major product, calcium should only be available in half the amount of phosphorus [32].

Wu et al. [18] studied the grate combustion of bran, showing that Ca-based additives increased the released K/P (+8–30%), whereas kaolinite showed an opposite effect (−60%).[2] According to their simplified thermodynamic computations, when the molar ratio of the released K/P is below 1, KPO_3 (Table 2) and $P_4O_{10}(g)$ are the main inorganic species above 500 °C. If flue gas temperature in the convective section is below 800 °C, a powdery, not sticking and easily removable deposit buildup is expected on the superheaters. When the molar ratio of the released K/P is greater than 1, below 500 °C, the released KPO_3 and $P_4O_{10}(g)$ may be converted to $H_3PO_4(l)$ which can cause low temperature fouling issues. These can be reduced by increasing the molar ratio of the released K/P to above 2 and using kaolinite for potassium retention in the bottom ash.

[2] A great reduction of the release of K is evidenced whereas the effect on P is insignificant [18].

Table 3
Some indices for a first prediction of ash-related issues in combustion [27–30].

Index	Qualitative risk
(1) $\frac{P+K+Si}{Ca+Mg}$	Indication of the ash-sintering temperature tendencies [28–30]
(2) K + Na + Zn + Pb + Cd	Aerosol formation potential (mg/kg d.b.) [27,28]
(3) $\frac{Cl+2S}{K+Na}$	Indication concerning HCl and SO_x content in the combustion products [27,28]
(4) $\frac{2S}{Cl}$	Indication of KCl sulphation, which could reduce the corrosion risk [27,28]
(5) $\frac{Ca}{S+1.5P}$	Indication of the S adsorption [27]

According to present knowledge, not all the potassium content is active in the ash chemistry; for example, potassium feldspar is not-reactive and harmless in combustion [27]. The alkalis that are soluble at a pH of 3 in the fuel leaching process can be assumed especially prone to deposition on convective heat exchangers [34]. Analogously, calcium is present in several silicate minerals in biomass, quite inert under combustion conditions. This fraction is insoluble in the selective leaching tests [27,35]. The fraction of the total calcium content involved in the ash chemistry is assumed as the one leachable from the fuel at pH 1 [34]. The pH 3 fraction can be defined as the inorganic matter fraction leached in ultra-pure H_2O and 1.0 M $NH_4Ac(aq)$ solutions in the chemical fractionation. The pH 1 fraction can be defined as the inorganic matter fraction leached in ultra-pure H_2O, 1.0 M $NH_4Ac(aq)$ and 1.0 M HCl(aq) solutions in the chemical fractionation.

Within our work, three improved molar quantities to characterise the high-P fuels[3] fouling are proposed, based on the analysis of the K_2O–CaO–P_2O_5 ternary system and global reactions Eq. (1)–(3), on the combination of the reported indices from Grimm [15], Piotrowska [24], Søresen et al. [25,32,33] and Wu et al. [18], and on the mentioned additional information from the chemical fractionation.

- $\frac{P}{(K_{pH3}+Na_{pH3})}$ $\left[\frac{mol}{mol}\right]$. A value higher than 0.4–0.5 corresponds to a high influence of P in the ash interactions.
- $\frac{P}{(Ca_{pH1}+Mg_{pH1})}$ $\left[\frac{mol}{mol}\right]$. A value higher than 1.0 could evidence the risk of formation of alkali–phosphates.
- $\frac{(Ca_{pH1}+Mg_{pH1})}{(K_{pH3}+Na_{pH3})}$ $\left[\frac{mol}{mol}\right]$. A value higher than 1.0, for P-rich fuels, could indicate high probability of formation of K–Ca–phosphates ternary phases [19].

For the reactive potassium and sodium contents, only the fraction of the oxides that has not reacted to silicates should be taken into account. However the competition between P and Si for reacting with K^+, Mg^{2+} and Ca^{2+} seems not fully understood, as previously mentioned [20,23]. Since the focus is the fouling, concerning the phosphorus content, only the fraction released from the fuel bed to fly ash (and not the one retained in the residual ash) should be taken into account.[4] As for potassium, high combustion temperatures seem to enhance the phosphorus volatilisation [36].

[3] Defined, for example, as a fuel with a P concentration in the ash higher than 1200 mg/kg (of fuel, dry basis) and with $P/(K_{pH3} + Na_{pH3}) > 0.2$.

[4] As an example, the phosphorus fraction released for poplar and brassica energy crops combustion was quantified to much below 20% [36]; on the contrary in case of bran combustion 60–70% of phosphorus content was released during combustion in the temperature range 900—1100 °C [18]. For agricultural residues the leachability of phosphorus in water and ammonium acetate in the fractionation process spans between 70% and 100% [35].

By the combination of these ratios, different limit scenarios can be analysed. Besides, it could be possible to evaluate in a preliminary simplified strategy (Fig. 1) whether potassium, calcium and phosphorus could be included in ternary alkali–alkaline earths–phosphates which have a positive effect concerning fouling, mainly by mitigating the formation of low melting temperatures potassium phosphates, chlorides and sulphates.

In case of scenario (a) a severe fouling behaviour is expected because, theoretically, alkali can react with P, Cl and S compounds forming fouling alkali phosphates, chlorides and sulphates. Also in case of scenario (b) a severe fouling behaviour is expected, however, the molar amount of alkaline earth metals is higher than the phosphorus content, increasing the probability of formation of high melting temperature K–Ca/Mg–P phases. In case of scenario (c), a severe fouling behaviour is expected since alkali phosphates are expected to be formed (preferential interaction with K). When looking at scenario (d), a medium fouling behaviour is expected because, theoretically, alkali can react with other species than phosphorus, forming alkali chlorides and sulphates. A relatively low occurrence of alkali phosphates is expected; alkali chlorides and sulphates are expected in less extent with respect to the scenario (b). If considering the scenario (e), theoretically, most of the alkali can react with Ca, Mg and P. A relatively low occurrence of alkali phosphates is expected, and alkali chlorides and sulphates are expected in less extent with respect to the case described in (d). However, P-compounds in the flue gas (i.e. H_3PO_4) should be monitored, because they could cause low temperature deposition problems [18]. This characterisation strategy should not be used without modifications in case of high silica fuels, because of the possibility of forming low melting points Ca–P–silicates [14], not investigated here because of the low quantities of Si in the sunflower hulls.

Following this approach, additives could be used to modify the elemental release (i.e. kaolinite) and to enhance the formation of specific phases (i.e. phosphorus and active calcium compounds), moving towards the scenarios (d) and (e). This strategy is expected to be helpful to evaluate possible countermeasures to hard fouling issues and to understand experimental outcomes presented in the following sections.

2.2. The drop tube furnace

In the last years, different studies about biomass fuel combustion performances have been performed in Drop Tube Reactors or Furnaces (DTF) [37,38]. In the frame of the this study, an experimental campaign took place in a DTF [5]. The DTF jointly developed by Laborelec and UCL is depicted in Fig. 2. Its main component is a 6 m-high vertical tube (17.8 cm ID) heated by electrical resistances. The furnace is composed of six electrical modules, of which the temperatures are independently regulated. The maximum temperature reached by the modules is 1300 °C. The metal alloy tube used in this study can withstand temperature up to 1100 °C. It is equipped with six pairs of welded ports, for easy injection or sampling of particles, as well as insertion of deposition probes. One additional visualisation port is installed at the bottom of the tube in order to have visual access to any deposition probe inserted in the lower pair of horizontal ports. For application up to 1300 °C, the alloy vertical tube can be replaced by a ceramic tube. The electrical modules can be easily opened for replacement of the tube or for maintenance, due to their unique half-shelf design, depicted in Fig. 3. The particles are dropped in the tube by gravity or are sucked in by an ejector and entrained in a compressed air flow. The mass flow rate is controlled by a vibrating plate. A gas burner can deliver flue gases to the vertical tube in order to control the combustion atmosphere. The deposition probes inserted horizontally through the ports are cooled by air or water, and are equipped with thermocouples welded on their surface (flash welding) for an accurate control of their surface temperature.

2.3. Experimental conditions

Six fuels have been considered for the experimental part of this work, namely RAW, PA1, PA2, PA3, PA4, PA3c. The main parameters for the conducted experiments are described in Table 4. The fuel RAW is sunflower hulls. The fuels PA1 to PA4 are sunflower hulls with an increasing concentration of phosphoric acid H_3PO_4 (PA) 85% aqueous solution as additive, in order to obtain different P/K ratios in the fuel. The fuel PA3c is sunflower hulls with a specific addition of phosphoric acid and calcium carbonate. The PA solution was diluted with water to get a final volume of 1 L of injected liquid for 15 kg of solid fuel. Limestone powder ($CaCO_3$) (>98%, Fisher Scientific) was added to reach a specific P/Ca ratio in the fuel composition (PA3c). The PA impregnation and the limestone addition (premixed) to the fuel was achieved in a cement mixer. For each experiment the fuel batch was inserted in the mixer for about 1 h. The measured P/K ratio of the fuel with PA addition was shown to be in good agreement with the targeted P/K ratio. Each fuel has been tested in the furnace. For each test, the biomass flow rate was set to 1.25 kg/h and about 5 kg of sunflower hulls fuel were burned. The DTF was fed with milled and sieved sunflower hulls with a particle mean size below 2 mm (aspect ratio 5–6).

The DTF operating parameters have been kept constant for all the tests. The temperature of each heating module was set in order to mimic the conditions seen by a particle before depositing on the economiser convective section (medium–low temperature) of a boiler (see Table 5). A deposition probe (25.4 mm diameter) was inserted in the horizontal port of the penultimate module and cooled using air in order to maintain a temperature of 200 ± 30 °C on its surface. Then the probe was removed and the deposits analysed. In this test campaign, the HCl and SO_2 concentrations in the flue gases were not monitored, being beyond the scope of this work.

3. Results and discussion

3.1. Fuel characterisation

The fuels tested were characterised with XRF analysis and the results are presented in Table 6 and Fig. 4. The variations among the samples composition could be explained: (1) considering the non homogeneity of the inorganic compounds distribution within the fuel matrix[5]), (2) considering the mixing with additives.

Chemical fractionation results for the PA3c case is reported in Figs. 5 and 6. The higher concentration of calcium and potassium in the ash with respect to the sample analysed, and for which the concentrations are reported in Table 6, might be explained considering inhomogeneity in the fuel batch and measurement errors. In the sample analysed, calcium is mainly acid leachable. The majority of the magnesium, phosphorus and potassium contents are water-soluble (about 90%). The high solubility of sulphur and phosphorus indicates the presence of alkali sulphates and phosphates. The insoluble part of sulphur indicates the presence of organically bonded sulphur.

The chemical fractionation for a RAW case sample was performed and the results are coherent with outcomes available in databases (not shown here). The addition of phosphoric acid causes an increase in the phosphorus content (as well as for sodium, present in the additive in a small quantity, <200 ppm). Almost all the

[5] For example, for calcium and sodium the concentrations in two samples of the same fuel (without PA addition) varied in the range ±35%.

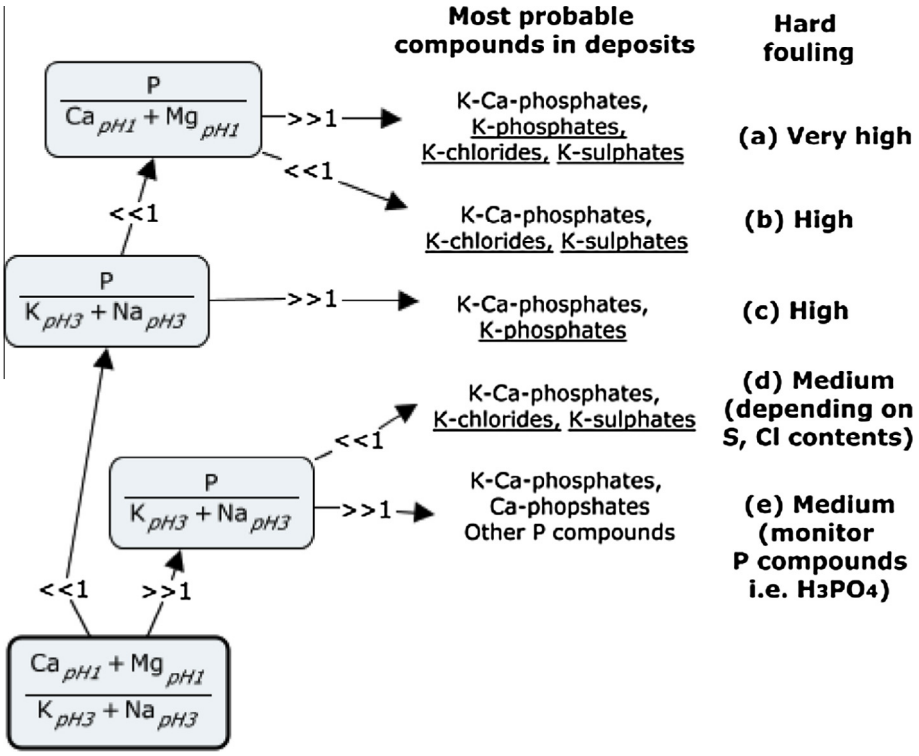

Fig. 1. Qualitative characterisation of the fouling propensity of high-P fuels. For case (e) low temperature deposition, not related to alkali but to the other P-compounds should be monitored.

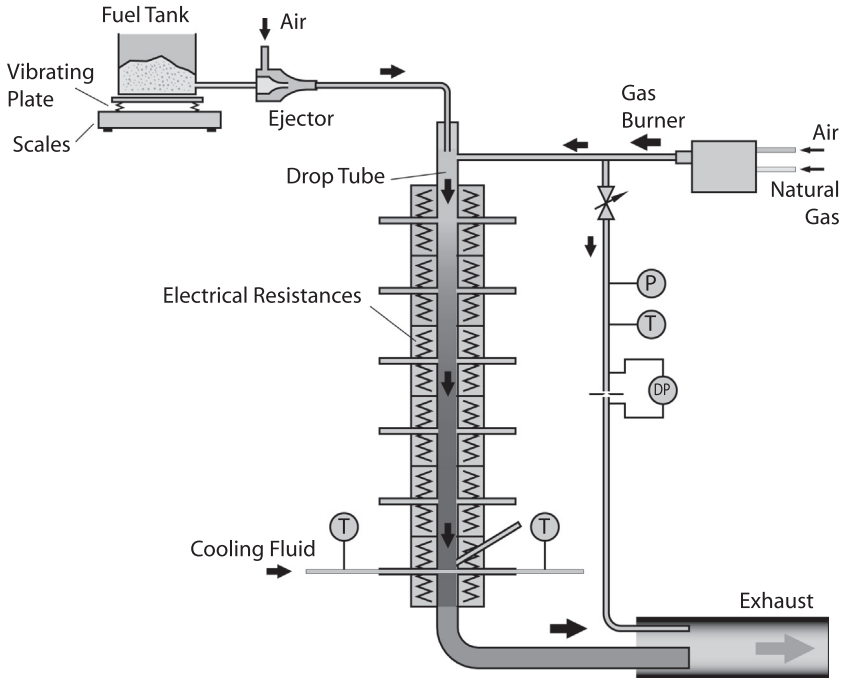

Fig. 2. Schematic of the drop tube furnace [5].

phosphorus added is found in the solubles fractions. As a partial conclusion, for the sunflower hulls analysed, the potassium and the phosphorus contents soluble at pH = 3 corresponds to the total contents. All the calcium in the fuel is soluble at pH = 1.

The majority of phosphorus in sunflower hulls is expected to be present as phytic acid or phytate if combined with other inorganic elements such as K, Mg, Ca, as is suggested for seed-originated biomass [18]. According to test performed for bran combustion [18], the elemental release of P in such an association happens in the temperature range 850–1100 °C, mainly forming KPO_3, which has a melting point of about 800 °C (Table 2).

The molar ratios introduced beforehand (see Table 3) were computed for all the tested fuels. The results are presented in Table 7. According to this first assessment, the probability of

Fig. 3. Laborelec–UCL drop tube furnace, with opened electrical modules, in order to access the vertical tube [5,12].

Table 4
Measured molar quantities in the fuel for the experimental campaign.

Experiment	P/Ca (mol/mol)	P/K (mol/mol)
Raw s. hulls [RAW]	0.69 ± 0.06	0.29 ± 0.08
PA addition [PA1]	2.00 ± 0.06	0.85 ± 0.08
PA addition [PA2]	3.54 ± 0.06	1.44 ± 0.08
PA addition [PA3]	4.80 ± 0.06	1.96 ± 0.08
PA addition [PA4]	7.61 ± 0.06	3.09 ± 0.08
PA, $CaCO_3$ addition [PA3c]	1.26 ± 0.06	1.96 ± 0.08

Table 5
Target and actual temperature for each of the 6 modules of the DTF, and for the probe surface.

DTF module	Target T (°C)	Actual T (°C)
Module 1 (top)	900	900 ± 6
Module 2	900	900 ± 4
Module 3	800	800 ± 2
Module 4	700	700 ± 1
Module 5	600	600 ± 1
Module 6 (bottom)	500	500 ± 4
Probe surface	200	200 ± 30

fouling is high. A high alkali concentration in the gas phase is expected. The silica content measured is low, indicating that high temperature fouling by molten alkali-silicate particles should present a low risk. The amounts of potassium and sodium with respect to the alkaline earth metals, which can increase the ash components melting temperatures in the bottom ash fraction, is relatively high. The coarse and fine fly ash emissions in the gas phase are

Table 6
Analyses of fuels tested (all fuels analysed, only the RAW, PA2, PA4, PA3c cases are here reported). Er (%) relative error in percent (RAW, PA2, PA4). (PHY2*) Median values from Phyllis 2 database (ECN): 3 samples. d.b.: dry basis. a.r. as received. daf: dry and ash free basis. n.a.: not available. LHV reported as (MJ/kg d.b.).

	Er (%)	RAW	PA2	PA4	PA3c	PHY2*
Sunflower hulls						
LHV	±0.5	19.0	19.0	18.6	19.0	19.4
M (% a.r.)	±2.0	12.2	16.5	16.0	8.1	10.5
Ash (% d.b.)	±2.0	3.0	3.5	4.9	7.4	3.8
C ($\%_{daf}$)	±0.6	50.5	49.8	48.4	49.4	51.1
H ($\%_{daf}$)	±2.0	6.0	6.0	5.9	5.9	6.1
O (diff.)		42.5	43.3	44.8	43.4	42.7
N ($\%_{daf}$)	±3.0	0.9	0.9	0.9	0.8	0.1
Ultimate analysis (mg/kg dry fuel)						
S	±3	1538	1601	1750	1769	2200
Cl	±10	764	765	641	752	*n.a.*
Ca	±2	2644	2073	2123	8049	3475
Mg	±8	1742	1797	2213	1990	1707
Al	±5	169	285	487	355	109
Si	±6	108	108	108	108	108
Fe	±6	223	119	112	119	1491
Mn	±11	28	17	23	105	80
P	±4	1410	5673	12481	7855	1366
K	±4	6126	4964	5097	5056	10864
Na	±8	653	994	1573	1217	100
Cu	±25	9	8	7	9	*n.a.*
Zn	±10	27	20	18	20	*n.a.*
Pb	±10	7	<1	<1	<1	*n.a.*
Cd	±30	4	3	3	7	*n.a.*
Ash melting behaviour						
IDT (°C)[a]	*n.a.*	*n.a.*	*n.a.*	*n.a.*	*n.a.*	940

[a] Initial Deformation Temperature from Phyllis 2 database (ECN).

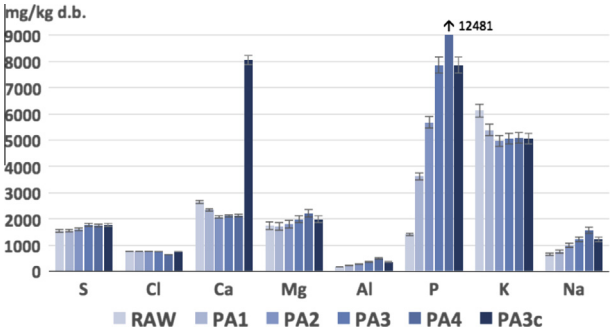

Fig. 4. Inorganic element concentrations in the different fuels tested.

expected to be medium-to-high. In particular, there is a high risk of formation of SO_x (relatively high sulphur content for a biomass fuel) and HCl, which can further react in the gas phase and in the deposits to form condensed KCl. A high sulphur to chlorine ratio is an indication of the possibility to have the sulphation of the chlorinated deposits, reducing the risk of corrosion [27,28]. However, alkaline earth metals can react with sulphur and with phosphorus, globally reducing its availability for the alkali chlorides sulphation.

Concerning the P-role, the strategy introduced in the previous section (Fig. 1) is applied. The results are presented in Table 8. All the potassium and sodium contents are considered as reactive. All the calcium and magnesium are considered as reactive, since the very low occurrence of silicate minerals in the sunflower hulls, and in coherence with selective leaching. As the split between bottom and fly ash cannot be investigated in an entrained flow DTF, all the phosphorus in the ash is considered available for the reactions and the deposition.

According to these results (Table 8), three preliminary types of information can be retained:

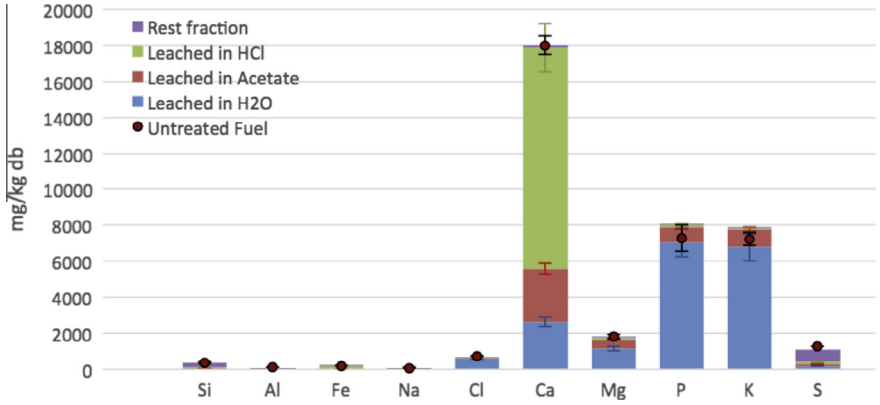

Fig. 5. Chemical fractionation results for a sample of the PA3c fuel batch.

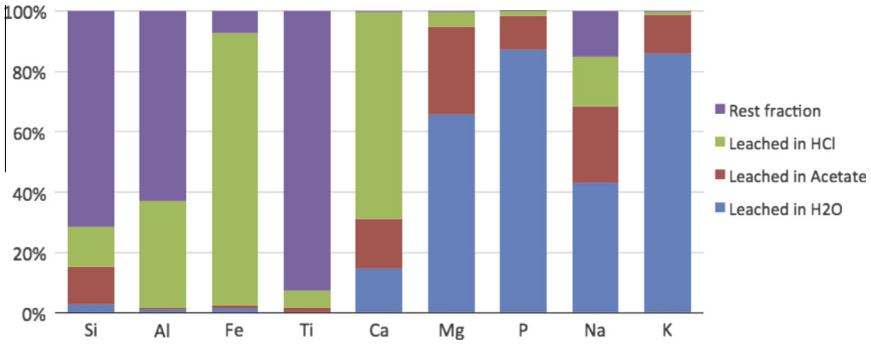

Fig. 6. Chemical fractionation results for a sample of the PA3c fuel batch (relative fractions).

Table 7
First prediction of ash issues in combustion of the considered fuels.

Index	Value RAW/PA2/PA3c/PA4
$\frac{P+K+Si}{Ca+Mg}$	1.5/2.5/1.4/3.7
K + Na + Zn + Pb + Cd	6817/5981/5986/6691
$\frac{Cl+2S}{K+Na}$	0.6/0.7/0.7/0.6
$\frac{2S}{Cl}$	4.4/4.6/4.2/6.0
$\frac{Ca}{S+1.5P}$	0.6/0.2/0.8/0.1

Table 8
Key molar indices concerning the P-role in the sintering propensity for the fuels analysed.

	$\frac{(Ca_{pH1}+Mg_{pH1})}{(K_{pH3}+Na_{pH3})}$ (mol/mol)	$\frac{P}{(K_{pH3}+Na_{pH3})}$ (mol/mol)	$\frac{P}{(Ca_{pH1}+Mg_{pH1})}$ (mol/mol)	Case (Fig. 1)
RAW	0.74 ± 0.09	0.25 ± 0.08	0.33 ± 0.08	b
PA1	0.75 ± 0.09	0.69 ± 0.08	0.91 ± 0.09	b
PA2	0.74 ± 0.10	1.08 ± 0.09	1.46 ± 0.09	c
PA3	0.74 ± 0.10	1.39 ± 0.09	1.88 ± 0.09	c
PA4	0.72 ± 0.10	2.03 ± 0.09	2.80 ± 0.09	c
PA3c	1.55 ± 0.09	1.39 ± 0.09	0.90 ± 0.09	e

1. For the RAW and PA1 cases theoretically, the phosphorus molar content, even if totally available, would be not sufficient to trap the reactive alkali in high melting temperature ternary phases. For the PA2, PA3, PA4 cases, the phosphorus could, theoretically, capture most of the alkali metals in ternary phases.
2. For all the fuels analysed apart from PA3c, the alkali earths molar content is lower than alkali metals molar content. Concerning the P-role, even if part of the potassium could be trap in alkali–alkaline earths–phosphate phases, there is a high probability that alkali metals react with sulphates and chlorides.
3. For all the cases apart form the RAW and PA3c samples, the phosphorus over the alkaline earth metals content in the fuel samples is higher than 1, with high risk of formation of low melting alkali phosphates.

As a summary for the PA2/PA3/PA4 cases respectively, a high/very high/very high sticky fouling behaviour is expected. Considering the PA1 case with respect to the RAW test, an increased amount of the phosphorus with respect to the alkali metals and alkaline earths metals is present. With respect to the RAW test, an increased amount of the phase K–Ca–phosphates could be formed. The RAW/PA1 cases are expected to have respectively a high/high fouling propensity. The case PA3c is expected to show the lowest rate of build up on the deposition probe, mainly formed by loose bounded deposits where the alkali–alkaline earths–phosphate phases are dominant; this case is represented by the scenario e (medium) in Fig. 1. The deposition tests visual and SEM–EDX analyses are presented in the next sections.

3.2. Visual inspections

The six deposition probes were visually analysed. The windward views of the deposition are presented in Fig. 7. Two different layers were observed on the deposition probes: (1) a loosely bounded coarse outer layer, essentially on the windward side of the probe, (2) a smooth and uniform inner layer covering the probe.

The outer layer was initially greyish/white (RAW, PA3c) and turned darker from PA1 to PA3, until being black for the PA4

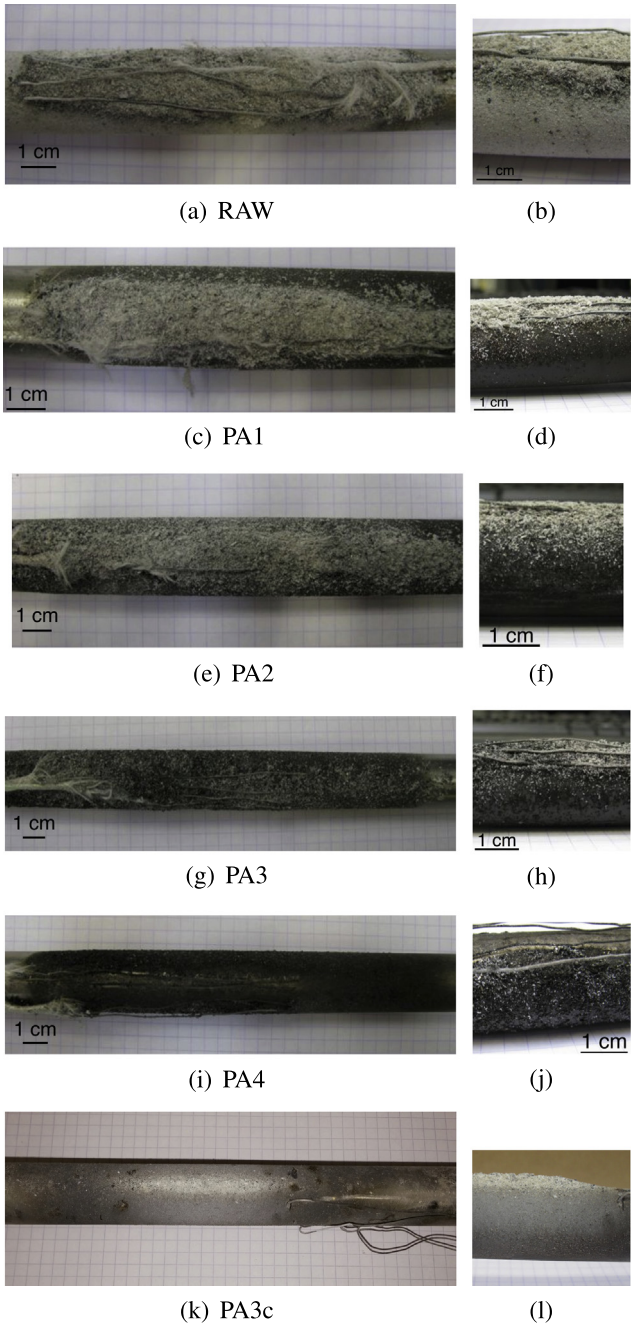

Fig. 7. Windward views of the deposition probes after deposition tests for each tested fuel sample. On the right side, details of the probes. The wires are the thermocouples used to control the probe surface temperature.

experiment. The layer was made of inertial impaction particles, easily removed by gravity. The particles seemed to be coarser and larger from PA1 to PA4 (about 1 mm diameter). This could be related to the formation of a high melting temperature K–Ca–phosphates ternary phase which could form seeds for heterogeneous condensation and the formation of larger ash particles in the flue gas. For the PA3 and PA4 experiments, the outer loosely bounded layer seemed to be reduced in thickness. In the PA3c experiment the outer layer seems constituted of inert greyish/white relatively small particles.

The inner, sticky, layer seemed to turn darker as the PA addition increased. The inner layer of the PA3c case seems less uniform and dark, and visually similar to the PA2 case. The layer for the RAW experiment has probably occurred by a condensation mechanism (smooth, thick and uniform). The layer structure for the experiments with PA addition looked more porous, probably made of a mix of particles and of condensed matter, also harder to remove than the greyish/white condensates (KCl and K_2SO_4 are expected) from the RAW experiment. This could be related to the formation of high melting temperature K–Ca–phosphates ternary phases, low melting temperature alkali phosphates and phosphoric acid condensate [18].

3.3. SEM–EDX analysis

SEM–EDX analyses were performed on the recovered deposits on a representative area[6] of about 1 mm^2, allowing for a semi-quantitative assessment of the elementary composition of the samples. For each of the six probes, two different ash samples were analysed: (1) a sample was taken on the probe itself, including the inner sticky deposition layer as well as some inertial impaction particles and (2) another sample was taken on the loose bounded particle deposits, which collided the probe due to the inertial impaction mechanism. The inorganic compositions of both the inner and outer layers were measured in large representative zones, as well as on specific points of interest, see Table 9. The fate of the key inorganic elements is discussed in the following, for each experiments, based on the tendencies presented in Fig. 8.

Sulphur (S) and chlorine (Cl) concentrations did not exceed more than 5% in the outer layers of the different experiments and not more than 10% in the inner layers (see Fig. 8). S and Cl present higher concentrations in the same spots in the inner deposition layer, in the form of alkali sulphate K_2SO_4 and KCl(s), given the high concentration of K in all the zones where S and Cl are to be found. The KCl compounds in the inner layer are expected to be formed by heterogeneous condensation [21,39,40]. The outer deposition layers of the PA3 and PA4 experiments showed the presence of zones with high S concentrations (>20%) combined with low Cl concentrations (<3%). As a very high Ca content is measured in those zones (>40%), sulphur is supposed to be present as calcium sulphate. In general, S and Cl contents seem to decrease in the inner and outer deposition layers with increasing PA addition (see Fig. 8). This could be explained considering the preferential association of K with P instead of with Cl and S species. Cl and S will then tend to stay in higher concentrations in the flue gas as HCl and SO_2, instead of depositing on the probe. The reduction of the Cl content in the deposits is especially favourable because of the corrosive character of KCl compounds. Interestingly, the S and Cl contents in the inner and outer layers seem to converge with an increased phosphorus content in the fuel (see Fig. 8). Sulphur and chlorine concentrations in the PA3c case deposits are low relatively to P and Ca contents, and not significantly different from case PA3, confirming the preferential association of K with P and Ca instead of Cl and S species. However, the spot analysis showed that some particles from the outer layer were most probably made of $CaCl_2$, which would motivate the higher chlorine concentration with respect to the PA4 and PA3 cases (see Fig. 8). $CaCl_2$ has a melting point of approximately 775 °C and could be formed according to the reaction (6) [35]:

$$CaO(s) + 2HCl(g) \rightleftharpoons CaCl_2(g,l) + H_2O(g) \quad (6)$$

The phosphorus concentration increases in both inner and outer deposition layers when increasing the PA addition (from 5% in the RAW experiment to more than 40% in the PA4 experiment, see Fig. 8). In the inner layer of the RAW experiment, the phosphorus

[6] Avoiding the boundaries of the probe deposition area.

Table 9
Molar concentrations of inorganic elements of some selected locations in the deposition layers analysed. Not all samples analysed are reported. For selected samples, the composition of the whole analysed area is given (Sum spectrum), as well as for some specific zones of interest (Spectrum). All results in molar %.

	Na	Mg	Al	Si	P	S	Cl	K	Ca	Fe	Cu	Zn	W
RAW experiment, outer layer (inert impaction particles)													
Sum spectrum	0.00	25.76	0.15	1.73	6.13	4.03	3.26	34.83	27.06	0.32	0.59	0.49	0.00
PA1 experiment, outer layer (inert impaction particles)													
Sum spectrum	0.00	14.51	0.34	1.63	22.05	3.24	1.65	37.20	21.44	0.46	0.35	0.31	0.00
Spectrum	4.02	2.75	17.11	42.61	8.07	0.91	0.45	18.15	8.68	0.49	0.30	0.14	0.00
Spectrum	0.00	9.43	0.81	2.68	38.23	0.58	0.45	36.77	12.79	0.76	0.21	0.00	0.00
PA3, inner layer													
Sum spectrum	0.00	9.49	0.27	0.33	35.95	2.93	5.00	33.95	21.63	0.58	0.79	0.64	0.62
Spectrum	0.00	6.15	0.39	0.60	18.66	2.20	16.16	42.57	13.88	0.42	0.77	0.63	0.00
PA3c, inner layer													
Sum spectrum	0.00	4.98	0.00	1.20	19.49	3.64	7.41	22.45	42.10	0.26	0.33	0.00	0.00

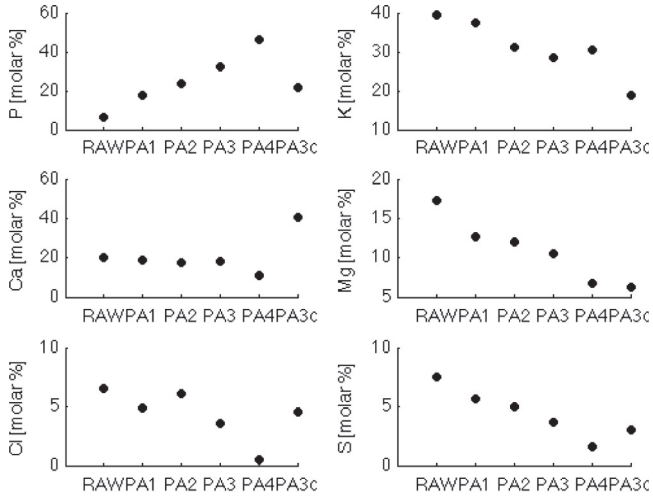

(a) Total deposit compositions

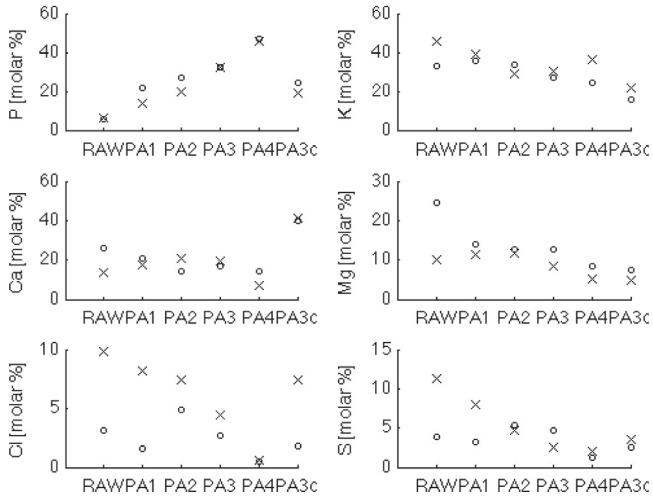

(b) Inner and outer layer compositions

Fig. 8. (a) Inorganic composition for the inner and outer deposition layers collected. (b) Inorganic composition for the inner layer (crosses) and the outer layer (circles) of the deposits collected in the experiments.

content is quite low. In K-rich zones (the largest areas of the condensed deposits), the potassium seems to be mainly associated with Cl and S (about 10% total weight relative percentage).

In the inner layer of the PA1 experiment, slightly less KCl and K_2SO_4 condensates are present, seen the lower K, S, Cl concentrations in Fig. 8. The outer layer of the PA1 experiment is richer in Ca and P, revealing the possible presence of a higher concentration of K–Ca–phosphates ternary phase. The phosphorus concentration in ash increased for the PA2 and PA3 cases: in both the removed layers in the form of K–Ca–phosphates ternary phase and alkali phosphates. Potassium phosphates are expected to occur by heterogeneous condensation on K–Ca–phosphates seed particles, since both K–Ca–phosphates ternary phases and K–phosphate phases are found in the same zone.

The phosphorus concentration increased by more than 10% between the PA3 and the PA4 tests (see Fig. 8). Both in the inner and outer layers of the PA4 experiment, deposits are dominated by molten potassium phosphate compounds. In the outer layer, the shape of the P-rich and K-rich zones is circular, a hint for condensate species. Alkali phosphates seem to have condensed on seeds before those seeds inertially impacted the outer layer of the deposition probe. For the PA3c case, the lowest concentration of potassium is measured, among the six tests (see Fig. 8). Most of potassium is found in the same spots as is phosphorus, in detriment to chlorine and sulphur. Few larger particles (about 50 μm), most probably made of K–Ca–phosphates, are found and probably acted like a seed for heterogeneous condensation of K–phosphate. Some chlorine and phosphorus rich zones, with low concentration of K but with high concentration of Ca or Mg, are also present. In the outer layer, the deposits analysis shows that phosphorus is mainly associated first to K, and then reacting with Ca, because K, P and Ca are found in high concentrations in the same spots (Fig. 9).

To summarise the experimental campaign outcomes, the addition of phosphoric acid increases the phosphorus concentration in the inner and in the outer ash deposition layers. Alkali sulphates and chlorides are reduced and a K–Ca/Mg–phosphates ternary phase is observed in both deposition layers already with small PA additions. The occurrence of this ternary phase replace some of the condensate-type deposition layer by a particulate-type layer. Nevertheless, for high concentrations of phosphorus in the gas phase, an increased amount of partially melt potassium phosphate and other phosphorus compounds is observed. In the PA3 and PA4 experimental sets, two mechanisms could have occurred: in the flue gas, the potassium phosphates could heterogeneously condense on seed particles, increasing the agglomeration and forming large, higher inertia,[7] particles; in the deposit, the partially melt layer probably acts as a glue for ash particles occurring by inertial impaction to stick on the deposition probe. This could explain the larger size of the impacted particles in the PA3 and PA4 experiments and the smaller amount of loose deposits. Finally, for the PA3c case, an increased amount of coarse, loosely bounded outer layer particles,

[7] Therefore with higher propensity to bounce off the probe after their impaction.

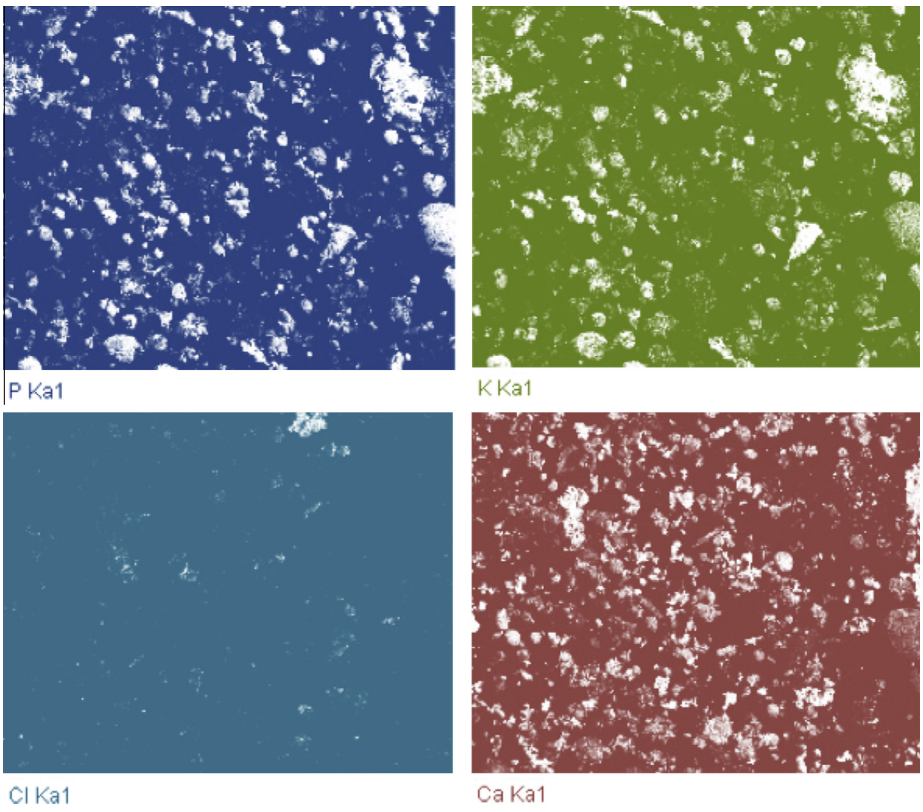

Fig. 9. SEM–EDX images for P, K, Cl, Ca of a representative area (1.7 mm^2) of the outer layer particles (removable by gravity) of the case PA3c.

mainly made of K–Ca/Mg–phosphates ternary phase is observed. The occurrence of this ternary phase, easier to remove from the probe, is maximised in this case, due to the higher availability of calcium. During the PA3c test, calcium chloride is also formed.

The experimental outcomes confirm the trends identified with the preliminary characterisation strategy (see Fig. 1). Due to an increased P content, K is captured in phosphate phases, due to an increased Ca content, the formation of K–Ca/Mg–phosphates ternary phase is maximised, reducing the occurrence in the deposits of S- and Cl-compounds and the sticky fouling behaviour.

4. Conclusions

During high-P solid biomass fuel combustion, part of the K and P is released and involves in complex interactions with other ash forming elements. Previous studies have shown the great influence of phosphorus on the ash deposition behaviour, even though the exact phosphorus-related deposition mechanisms are still not completely understood.

A detailed literature review suggested to assess, in a simplified characterisation step, the high phosphorus fuel fouling behaviour with three molar quantities in the ash. The simplified strategy developed could be used for a preliminary characterisation of the fouling behaviour of high-P solid fuels and for a semi-quantitative assessment of the need for additives. Furthermore it could integrate thermodynamic equilibrium models outcomes, which however still suffer from a lack of data and results dependency on the database used for the calculations, especially for phosphorus compounds [13,23].

The experimental results show that increasing the fuel P-content allows to capture the alkali metals in alkali–alkaline earths–phosphates and alkali–phosphates phases, reducing the occurrence in the deposits of S- and Cl-compounds. Low melting temperature phases can be reduced enhancing the formation of coarser, high melting temperatures ash particles formed by K/Na–Ca/Mg–phosphates. The investigation suggests that sunflower hulls fouling could be reduced by an optimised addition of phosphorus and alkaline-earth metals additives, confirming the trends identified for logging residues and wheat straw [19], on the conditions that higher concentrations of acidic gases HCl, SO_2 can be tolerated [22]. The drop tube furnace experimental results confirm the tendencies identified in the preliminary characterisation strategy proposed. The characterisation strategy, based on three improved indices, can bring valuable information on the fouling propensity, when processing high-P solid fuels.

Further experimental work should be performed to assess the ash behaviour when co-firing a high-P fuel with a high-Ca fuel (e.g. bark) and to assess the effectiveness of calcium-based additives (i.e. $CaCO_3, CaOH_2, Ca(H_2PO_4)_2H_2O$) to minimise the rate of buildup for agro-residues with high phosphorus content. Improvements in the experimental outcomes would be reached with flue gas measurements in the DTF. Additional fundamental research should also investigate the phosphorus split between the bottom ash and fly ash.

Acknowledgements

Thanks are extended to Ir. Frank Roman for the support for the fuel procurement. Vyncke and Laborelec are acknowledged for the support for the samples analyses. The authors acknowledge the financial support of Electrabel ENGIE.

References

[1] El Bassam N. Handbook of bioenergy crops. London: Earthscan; 2010.
[2] Baxter LL, Miles TR, Miles Jr TR, Jenkins BM, Milne T, Dayton D, et al. Fuel Process Technol 1998;54(1):47–78.

[3] Jöller M. Fuel Process Technol 2007;88:1136–47.
[4] Stam AF, Livingston W, Cremers M, Brem G. Review of models and tools for slagging and fouling prediction for biomass cocombustion; 2009.
[5] Blondeau J. Numerical and experimental investigation of pulverised biomass combustion: modelling of particle pyrolysis and analysis of ash deposition, Ph. D. thesis, Université Catholique de Louvain; 2013.
[6] Teixeira P. Biomass Bioenergy 2012;39:192–203.
[7] Van Loo S, Koppejan S. The handbook of biomass combustion & cofiring. London: Earthscan; 2008.
[8] Obernberger I, Fluch J, Brunner T. Comparative characterization of high temperature aerosols in waste wood fired fixed bed and fluidized bed combustion systems. In: Proc of the 17th European biomass conference and exhibition; 2009.
[9] Jenkins BM, Baxter LL, Miles Jr TR. Fuel Process Technol 1998;54:17–46.
[10] Doshi V, Vuthaluru H, Korbee R, Kiel J. Fuel Process Technol 2009;90 (9):1148–56.
[11] Miles TR. Biomass Bioenergy 1996;10:125–38.
[12] Blondeau J, Ryckmans Y, Corbisier D. Characterization of sunflower husk ash deposition in a drop tube furnace. In: Proc of the 22nd European biomass conference and exhibition; 2014.
[13] Obernberger I. The present state and future development of industrial biomass combustion for heat and power generation. In: Proc of the ASME-ATI-UTI conference on thermal and environmental issues in energy systems; 2010.
[14] Piotrowska P. Fate of phosphorus during co-combustion of solid biofuels. In: Proceedings of the 20th international conference on fluidized bed combustion. Springer; 2009.
[15] Grimm A. Experimental studies of ash transformation processes in combustion of phosphorus-rich biomass fuels, Ph.D. thesis, Lulea University of Technology; 2012.
[16] Eriksson G. Fuel 2012;102:208–20.
[17] Billen P, Creemers B, Costa J, Van Caneghem J, Vandecasteele C. Biomass Bioenergy 2014:71–9.
[18] Wu H, Castro M, Pater AJ, Frandsen FJ, Glarborg P, Dam-Johansen K, et al. Energy Fuels 2011;25:2874–86.
[19] Grimm A. Energy Fuels 2012;26:3012–23.
[20] Boström D. Energy Fuels 2009;23:5184–90.
[21] Christensen K. J Aerosol Sci 1998;29:421–44.
[22] Boström D. Energy Fuels 2012;26:85–93.
[23] Billen P, Van Caneghem J, Vandecasteele C. Waste Biomass Valor 2014;5:879–92.
[24] Piotrowska P. Combustion properties of biomass residues rich in phosphorus, Ph.D. thesis, Abo Akademi; 2012.
[25] Castellino F. Deactivation of SCR catalysts by additives, Ph.D. thesis, Technical University of Denmark; 2008.
[26] Lindström E. Energy Fuels 2007;21:710–7.
[27] Strömberg B. Fuel handbook, swedish version translated Edition, Värmeforsk Service AB; 2006.
[28] Frandsen J, Glarborg P, Arendt Jensen P, Dam Johansen K, Boll Illerup J. Scientific tools for fuel characterization for clean and efficient biomass combustion, SciToBiCom final report, Tech rep, DTU, Abo Akademi University, BE2020+/Graz University of Technology, NTNU; 2013.
[29] Obernberger I. Energy Fuels 2014;28(2):1041–52.
[30] Sommersacher P, Brunner T, Obernberger I, Kienzl N, Kanzian W. Energy Fuels 2013:5192–206.
[31] Novakovic A, van Lith SC, Frandsen FJ, Jensen PA, Holgersen LB. Energy Fuels 2009;23:3423–8.
[32] Srensen L, Fjellerup J, Henriksen U. Method for reducing agglomeration, sintering and deposit formation in gasification and combustion of biomass, Google Patents, 2003, US Patent 6,615,751.
[33] Jensen PA, Sørensen L, Hu G, Holm J, Frandsen F, PSO Project: Biomass Dust Firing, DTU, Denmark.
[34] Zabetta EC, Barisic V, Mahanen J, Peltola K. Foster Wheeler Publication; 2012.
[35] Zevenhoven M, Yrjas P, Hupa M. Ash forming matter and ash related problems. In: Lackner M, Winter F, Agarwal AK, editors. Handbook of combustion. Solid Fuels, vol. 4. Weinheim: Wiley; 2010. Edition.
[36] Díaz Ramírez M, Frandsen FJ, Glarborg P, Sebastián F, Royo J. Fuel 2014:209–19.
[37] Biagini E, Cioni M, Tognotti L. Fuel 2005:1524–34.
[38] Septien S, Valin S, Peyrot M, Dupont C, Salvador S. Fuel 2014;121:216–24.
[39] Sengeløv L. Energy Fuels 2013;27:3283–9.
[40] Hindiyarti L. Fuel 2008;87:1591–600.